THE JOURNAL OF BIOLOGICAL CHEMISTRY VOL. 287, NO. 30, pp. 24941–24954, July 20, 2012

Transcriptional Regulation of the Protocadherin β Cluster during Her-2 Protein-induced Mammary Tumorigenesis Results from Altered *N*-Glycan Branching*[S]

Received for publication, April 4, 2012, and in revised form, May 24, 2012 Published, JBC Papers in Press, June 4, 2012, DOI 10.1074/jbc.M112.369355

Huabei Guo[‡§], Alison Nairn[‡§], Mitche dela Rosa[‡§], Tamas Nagy[¶], Shaying Zhao[‡], Kelley Moremen[‡§], and Michael Pierce[‡§‖1]

From the [‡]Department of Biochemistry and Molecular Biology, [§]Complex Carbohydrate Research Center, [¶]Department of Pathology, College of Veterinary Medicine, and [‖]Cancer Center, University of Georgia, Athens, Georgia 30602

Background: Her-2-induced mammary tumor onset is significantly delayed in *GnT-V* knock-out mice.
Results: The gene expression of the *Pcdhβ* cluster is up-regulated in her-2-induced tumors with *GnT-V* deletion.
Conclusion: Up-regulation of the *Pcdhβ* cluster is one of the mechanisms for the reduced her-2-mediated tumorigenesis resulting from *GnT-V* deletion.
Significance: Our findings shed new light on the molecular mechanisms of the effects of *GnT-V* on mammary tumorigenesis.

Changes in the levels of *N*-acetylglucosaminyltransferase V (*GnT-V*) can alter the function of several types of cell surface receptors and adhesion molecules by causing altered *N*-linked glycan branching. Using a her-2 mammary tumor mouse model, her-2 receptor signaling was down-regulated by *GnT-V* knock-out, resulting in a significant delay in the onset of her-2-induced mammary tumors. To identify the genes that contributed to this GnT-V regulation of early events in tumorigenesis, microarray analysis was performed using her-2 induced mammary tumors from wild-type and *GnT-V*-null mice. We found that 142 genes were aberrantly expressed (>2.0-fold) with 64 genes up-regulated and 78 genes down-regulated after deletion of *GnT-V*. Among differentially expressed genes, the expression of a subgroup of the cadherin superfamily, the protocadherin β (*Pcdhβ*) cluster, was up-regulated in *GnT-V*-null tumors. Altered expression of the *Pcdhβ* cluster in *GnT-V*-null tumors was not due to changes in promoter methylation; instead, impaired her-2-mediated signaling pathways were implicated at least in part resulting from reduced microRNA-21 expression. Overexpression of *Pcdhβ* genes inhibited tumor cell growth, decreased the proportion of tumor-initiating cells, and decreased tumor formation *in vivo*, demonstrating that expression of the *Pcdhβ* gene cluster can serve as an inhibitor of the transformed phenotype. Our results suggest the up-regulation of the *Pcdhβ* gene cluster as a mechanism for reduced her-2-mediated tumorigenesis resulting from *GnT-V* deletion.

Studies have shown that changes in *N*-glycan structures on specific receptors were associated with abnormal receptor-mediated phenotypes by affecting cell adhesion, migration, cell survival, and tumorigenesis (1). A glycan whose expression is often up-regulated during malignant transformation contains *N*-linked β(1,6)-acetylglucosamine synthesized by *N*-acetylglucosaminyltransferase V (*GnT-V*[2] or *Mgat5*; EC 2.4.1.155) (2, 3). Both *in vitro* and *in vivo* studies have implicated GnT-V in regulating tumorigenesis and invasiveness (4–9). Moreover, patients with colorectal or breast carcinomas that show expression of GnT-V glycan product have lowered 5-year survival rates (7, 10). Multiple cell surface receptors have been identified as substrates of GnT-V, including integrins (4, 6), cadherins (11, 12), and growth factor receptors (13, 14).

Her-2 (neu/ErbB2), a 185-kDa transmembrane glycoprotein and a member of the epidermal growth factor (EGF) receptor family, is overexpressed in ~15–30% of human breast cancer and has been correlated with poor prognosis of cancer patients and therapeutic resistance (15, 16). The oncogenic potential of her-2 in mammary tumorigenesis has been confirmed in transgenic mouse models with overexpression or mutation of *her-2* under the transcriptional control of the mouse mammary tumor virus promoter, and oncogenesis induced by her-2 in these transgenic mice has been shown to be quite similar to human breast cancer (17, 18). We recently showed that her-2 receptor signaling is modulated by GnT-V expression levels. Her-2-induced mammary tumor onset is significantly delayed in *GnT-V* knock-out mice coincident with the reversion of her-2-induced deregulation of acinar morphogenesis and a significantly reduced population of tumor-initiating cells (cancer stem cells) in isolated tumor cells with *GnT-V* deletion, resulting in reduced ability to form secondary tumors in NOD/SCID mice (9). These results indicate that GnT-V promotes mammary tumor development by regulating some early events during tumorigenesis.

In addition to altering growth factor receptor signaling, the function of cadherins is modulated by GnT-V expression levels. For example, knockdown of *GnT-V* reduces the expression of

* This work was supported, in whole or in part, by National Institutes of Health Grants U01CA128454 (to M. P.) and P41RR018502 (to M. P. and K. M.).
[S] This article contains supplemental Figs. 1–6 and Tables S1–S6.
[1] To whom correspondence should be addressed: Dept. of Biochemistry and Molecular Biology and Complex Carbohydrate Research Center, University of Georgia, 315 Riverbend Rd., Athens, GA 30602. Tel.: 706-542-1701; Fax: 706-542-1759; E-mail: hawkeye@uga.edu.

[2] The abbreviations used are: GnT-V, *N*-acetylglucosaminyltransferase V; NOD/SCID, non-obese diabetes/severe combined immunodeficiency; Pcdh, protocadherin; qRT-PCR, quantitative RT-PCR; miR, microRNA; phospho, phosphorylated; TSS, transcription start site.

β(1,6) branching on the extracellular EC2–3 domains of N-cadherin, increasing N-cadherin-mediated cell-cell adhesion (11), whereas the deletion of *GnT-V* increases E-cadherin localization in cell adhesion junctions and cell-cell adhesion in both polyoma middle-T and her-2-induced mammary tumors (9, 13). The cadherins constitute a superfamily of single pass transmembrane glycoproteins mediating calcium-dependent cell-cell adhesion that plays an essential role in regulating major cellular behaviors, including cell growth, motility, and differentiation (19, 20). Several subgroups of cadherins have been defined based on shared properties and sequence similarity, including classical cadherins and protocadherins (21). Protocadherins (*Pcdhs*) are divided into clustered and non-clustered groups based on their genomic structures. Three closely linked protocadherin gene clusters, *Pcdhα*, *Pcdhβ*, and *Pcdhγ*, have been identified in both mouse and human (22, 23). Unlike classical cadherins that have five extracellular domains, a transmembrane domain, and a conserved cytoplasmic domain, Pcdhs have six extracellular domains encoded by one large exon and distinct intracellular domains (24). Protocadherins are predominantly expressed in the nervous system and appear to play an important role in regulating neuron development (21). However, epigenetic aberrations of protocadherin gene clusters caused by hypermethylation have been identified recently in some human tumors, including breast cancer (25–28), indicating that *Pcdh* genes may serve as tumor "suppressors" that can inhibit tumor development.

To identify the genes that could be contributive to early breast tumor progression regulated by GnT-V (9), microarray analysis was performed using mammary tumor tissues from *GnT-V* wild-type and knock-out her-2 mice, and qRT-PCR was used to confirm transcript differences. Here, we present evidence that members of the *Pcdhβ* gene cluster are implicated, functioning to suppress the malignant phenotype, in her-2-mediated mouse mammary tumorigenicity. We found that deletion of *GnT-V* caused enhanced gene expression of the *Pcdhβ* cluster in *GnT-V* knock-out tumors that contributes to the reduced her-2-induced tumorigenesis. Increased gene expression of the *Pcdhβ* cluster in *GnT-V* knock-out tumors was mediated by attenuated her-2-mediated signaling pathways caused by deletion of *GnT-V*. One of the downstream regulators of her-2 signaling, microRNA-21 (miR-21), was identified and implicated at least in part in the increased gene expression of *Pcdhβ* cluster.

EXPERIMENTAL PROCEDURES

Cell Lines and Materials—Human breast carcinoma cell lines MDA-MB231 and SK-BR3 were from the American Type Culture Collection (Manassas, VA). Mouse her-2 tumor cells with different *GnT-V* backgrounds were isolated from her-2 tumor tissues as described in our previous report (9). For silencing experiments, miRCURY locked nucleic acid-modified anti-miR-21 or control miRCURY knockdown oligonucleotides were purchased from Exiqon. Silencer® select neu/ErbB2 siRNA and scrambled control siRNA oligonucleotides were from Applied Biosystem (Ambion). pSuper vectors containing GnT-V siRNA and scrambled control siRNA were constructed and described in our previous report (14). 5-Aza-2′-deoxycytidine, PD98059, and wortmannin were purchased from Sigma; Lipofectamine™ 2000 reagent was from Invitrogen. Anti-Pcdhβ4 and -Pcdhβ7 were products of Abcam. Antibodies against ErbB2/neu, ERK, phospho-ERK, PKB, and phospho-PKB and HRP-labeled anti-rabbit IgG and anti-mouse IgG were from Santa Cruz Biotechnology. Anti-c-myc tag (clone 9E10) was from Millipore.

Mouse Breeding and Tumor Tissue Isolation—All procedures used for this study were approved by the Institutional Animal Care and Use Committee of the University. The *her-2*/*GnT-V*(+/+) and *her-2*/*GnT-V*(−/−) mice were produced by breeding *her-2*/*neu* transgenic mice with GnT-V knock-out mice and genotyped by PCR as our previously described (9). Mice with tumors were euthanized at 10 weeks after the first detection of a palpable tumor. Mammary tumor tissues were collected from three her-2 mice with wild-type *GnT-V*(+/+) (mouse identification numbers 2319, 2328, and 2323) and *GnT-V*-null (−/−) (mouse identification numbers 2318, 2205, and 2414) backgrounds, respectively; immediately frozen in liquid nitrogen; and stored at −80 °C.

Microarray—Total RNA was isolated from tumor tissues using TRIzol reagent and cleaned using RNeasy columns (Qiagen). Using a random hexamer incorporating a T7 promoter, double-stranded cDNA was synthesized from total RNA. cRNA was generated from the double-stranded cDNA template through an *in vitro* transcription reaction and purified using the Ambion WT Expression kit and sample cleanup module. cDNA was then regenerated through a random primed reverse transcription using a dNTP mixture containing dUTP. Fragmented and biotinylated cDNA was used for hybridization with an Affymetrix Mouse GeneChip® Gene 1.0 ST Array according to the manufacturer's protocol.

Expression Analysis—Gene expression alterations were determined using the PARTEK Genomics Suite. The CEL files were imported from the Affymetrix Expression Console and background-corrected and quantile-normalized, and probe summarization was performed using Robust Multichip Analysis (RMA). A gene summarization was performed on the data that estimates the intensity of individual genes by averaging the intensities of all the probe sets comprising the gene followed by an *n*-way analysis of variance using a mixed model and methods of moment to equate analysis of variance mean sum of squares to their expected values. The data were then analyzed using a two-sample *t* test for significance at $p = 0.05$ and a -fold change cutoff of 2.0. To assess the possible functional connections between the differentially expressed genes, a pathway analysis, which assesses statistically overrepresented functional terms within a list, was conducted using Ingenuity Pathways Analysis (IPA) for all comparisons. The probability that a specific set of genes has a significant number of members in a canonical pathway is assigned a *p* value, which is calculated by Fisher's exact test (right tailed). The *p* value indicates the probability of observing the fraction of the focus genes in the canonical pathway compared with the fraction expected by chance in the reference set with the assumption that each gene is equally likely to be selected by chance.

qRT-PCR Analysis—TRIzol was used to isolate total RNA from tumor tissues and cell lines. Reverse transcription reac-

tions were performed using cDNA synthesis kit (Bio-Rad). Primers used in the qRT-PCR analysis are listed in supplemental Table S1. Real time reactions were performed using the iQ™ SYBR Green Supermix (Bio-Rad) as reported previously (29). All PCRs were performed in triplicate samples and repeated at least two times.

Genomic DNA Purification, Bisulfite Modification, and Methylation-specific PCR—Purification and bisulfite treatment of genomic DNA samples were performed using the DNeasy Tissue kit and the EpiTect Bisulfite kit (Qiagen), respectively, according to the manufacturer's instructions. Methylation-specific PCR was carried out using the following cycling conditions: 95 °C for 5 min; 40 cycles at 95 °C for 30 s, 50 °C for 30 s, and 72 °C for 45 s; and a final cycle at 72 °C for 5 min. The primer sequences used for methylation-specific PCR are listed in supplemental Table S2. The PCR products were isolated on a 1.5% agarose gel and visualized by ethidium bromide staining.

Real Time PCR Detection of miR-21—Mature miR-21 was detected using the miR-Q method as described previously (30, 31). In brief, 500 ng of total RNA was used for reverse transcription of mature miR-21 using TaqMan reverse transcription reagents (Applied Biosystems) with a specific reverse primer (RT6-miR-21, tgtcaggcaaccgtattcaccgtgagtggttcaaca). The miR-cDNA generated was then quantitated using SYBR Green PCR Master Mix (Bio-Rad) with another specific primer (short-miR-21-rev, cgtcagatgtccgagtagagggggaacggcgtagcttatcagactga) and one pair of universal primers (MP-fw, tgtcaggcaaccgtattcacc and MP-rev, cgtcagatgtccgagtagag). The amplification was performed by a first step at 95 °C for 10 min followed by 40 cycles of 15 s at 95 °C, 10 s at 59 °C, and 20 s at 72 °C. Amplification of *Gapdh* was used as an internal control.

Construction of pcDNA3.1/myc-His/Pcdhβ Expression Plasmids and Cell Transfection—Mouse *Pcdhβ4* cDNA clone (clone identification number 6401988) and *Pcdhβ19* cDNA clone (clone identification number 9055902) were purchased from Source BioScience (Cambridge, UK). These cDNA clones were used as PCR templates to amplify the ORFs of *Pcdhβ4* and *Pcdhβ19* with the forward primer containing a HindIII site and the reverse primer containing an XbaI site. The sequences of forward and reverse primers were 5′-cccaagcttacaatggagacagcgcta-3′ and 5′-ctgtatctagaactattcaacatgt-3′, respectively, for *Pcdhβ4* and 5′-tggaagcttactatggagaatcaagag-3′ and 5′-acatctagaattacagtccctaaat-3′, respectively, for *Pcdhβ19*. The final PCR product was ligated into a pcDNA3.1/myc-His expression vector (Invitrogen) digested with HindIII and XbaI according to the manufacturer's instructions. The resulting vectors were confirmed by sequencing and digested with HindIII and XbaI to release the DNA fragment, which was inserted into the pcDNA3.1 vector upstream from the myc-His tags.

Cell transfections were performed in 6-well plates with Lipofectamine 2000 according to the manufacturer's instructions using 4 μg of recombinant plasmids. 24 h after transfection, cells were selected for 3 weeks using G418 (800 μg/ml), and nonclonal populations of transfected cells were used for all experiments.

Colony Formation and Anchorage-independent Growth Assay—For the colony formation assay, cells were transfected with 4 μg of expression plasmids in 6-well plates and transferred into 100-mm culture dishes the next day. Selection was performed 2 days after transfection with 800 μg/ml G418 for 2 weeks. Colonies were stained with crystal violet and counted in 5–10 random fields under a phase-contrast microscope.

An assay of cell growth in soft agar was performed using 24-well culture plates (27). The wells were coated with two layers of agar in different concentrations. The lower layer was 0.7% agar in 0.9% sodium chloride, whereas the upper layer was 0.35% soft agar in complete culture medium. 3×10^4 cells were added into the upper layers of the wells. Plates were incubated at 37 °C in 5% CO_2 for 2–3 weeks. Then the numbers of the colonies that developed in soft agar were counted in 5–10 random fields under a microscope.

Implantation of Tumor Cells in NOD/SCID Mice—All procedures were performed in accordance with the NIH Guide for the Care and Use of Laboratory Animals and were approved by the Institutional Animal Care and Use Committee of the University of Georgia. Subconfluent tumor cells were harvested and resuspended in serum-free Hanks' balanced salt solution in a 70-μl volume containing 2×10^6 cells. After NOD/SCID mice (The Jackson Laboratory) were anesthetized with isoflurane, a 70-μl single cell suspension mixed with 30 μl of Matrigel (BD Biosciences) was injected into flanks of mice of 6–8 weeks age using a 27-gauge needle (9). Tumor formation was monitored by palpation, and tumor size was measured with calipers once a week.

Western Blotting—Subconfluent cells were harvested and lysed. Total cell lysates containing 30 μg of protein were used for Western blotting as described in our earlier report (6).

ALDEFLUOR Assay—To detect tumor cells with high aldehyde dehydrogenase activity, the ALDEFLUOR assay was performed using an ALDEFLUOR kit from STEMCELL Technologies as described previously (9, 32). In brief, dissociated single cells (1×10^6 cells/ml) were incubated in ALDEFLUOR assay buffer containing aldehyde dehydrogenase substrate (1.5 μM) at 37 °C for 30 min. In each experiment, a fraction of cells was stained under identical conditions with a specific aldehyde dehydrogenase inhibitor, diethylaminobenzaldehyde (15 μM), as a negative control. After staining with propidium iodide, aldehyde dehydrogenase-positive (tumor-initiating cells) and -negative cells (non-tumor-initiating cells) were analyzed using flow cytometry.

Immunochemical and Fluorescent Staining—Immunochemical staining were performed using a VECTASTAIN® Elite ABC kit (Vector laboratories) following the manufacturer's instructions. For fluorescent staining, cells were cultured on chamber slides, fixed with 4% paraformaldehyde in PBS for 10 min, and permeabilized with 0.05% Triton X-100. After blocking with 10% goat serum, cells were stained with primary antibodies followed by incubation with secondary fluorescence-conjugated anti-mouse or rabbit IgG (1:250). After washing with PBS, the chamber slides were mounted, and the cells were subjected to fluorescence microscopy.

RESULTS

Microarray Analysis of Her-2-induced Mammary Tumors—We recently demonstrated that deletion of *GnT-V* reduces the size of the compartment of tumor-initiating cells in a her-2

mouse model, consequently leading to an inhibition of her-2-induced mammary tumor onset (9). To systematically study the mechanisms by which deletion of *GnT-V* inhibited her-2-induced tumor onset, microarray analyses were performed on the her-2-induced mammary tumors isolated from mice with wild-type (WT) and *GnT-V*-null (KO) genotypes. Three tumor tissues (T1–3) were collected, each from three her-2 mice with wild-type *GnT-V*(+/+) and *GnT-V*-null (−/−) backgrounds, respectively, and the *GnT-V* expression was confirmed by RT-PCR using total RNA (supplemental Fig. 1A). Using the normalized data from the Mouse GeneChip Gene 1.0 ST Array, gene lists were generated using the PARTEK Genomics Suite for differentially expressed genes in these two groups of tumors. There were 142 genes (0.4% of the total 35,556 genes) differentially expressed in *GnT-V* KO tumors compared with wild-type tumors using a 2-fold change as the ratio threshold. Among the 142 genes identified, 64 genes were up-regulated, and 78 genes were down-regulated (from 2.0- to 6.5-fold) (supplemental Table S3). Of the 142 differentially expressed genes, 57 genes (40.1%) were found to be significantly different ($p < 0.05$) (Table 1). An agglomerative clustering diagram (heat map) was generated from the microarray data of her-2 tumors based on the differentially expressed genes (Fig. 1*A* and supplemental Fig. 1B) in *GnT-V* KO tumors. Functional characterization of these differentially expressed genes by Ingenuity Pathways Analysis (IPA) classified them into different categories, including RNA damage and repair, cellular compromise, inflammatory response, and cell-to-cell signaling and interaction (supplemental Fig. 1B, left panel). The top 10 IPA-identified, differentially expressed genes (both up-regulated and down-regulated) are summarized in supplemental Table S4 and were validated by qRT-PCR as shown in supplemental Fig. 2.

Gene Expression of Pcdhβ Cluster Is Up-regulated in GnT-V KO Tumors—The functions of many cell surface receptors have been shown to be altered by the GnT-V expression level, including integrins (4, 6), cadherins (11, 12), and EGF family receptors (EGF receptor/ErbB1/her-1 and ErbB2/her-2) and TGFβ receptors (9, 13, 14). As listed in supplemental Table S5, compared with wild-type tumors, her-2-induced mammary tumors showed little change in the transcript abundances of other glycosyltransferases and lectins except for *Gcnt1*, the enzyme that synthesizes core 2-*O*-glycans. *Gcnt1* was significantly down-regulated (>3-fold) in *GnT-V*-null tumors based on the microarray data. However, *GnT-V* expression was reduced by only 2.1-fold in *GnT-V* KO tumors, although undetectable levels of both GnT-V mRNA and *N*-linked β(1,6) branching were observed by RT-PCR and leukocytic phytohemagglutinin staining, respectively (supplemental Fig. 1, A and D) (9), indicating either that some probes in the GnT-V probe set used in the microarray analysis target the areas of GnT-V mRNA that is transcribed from the non-deleted portions of the *GnT-V* gene (5) or that nonspecific hybridization generated by a few of the probes in the GnT-V probe set may have occurred. Among the 142 differentially expressed genes in *GnT-V* KO tumors, neither integrins nor growth factor receptors were observed, indicating that deletion of *GnT-V* had no detectable effects on the transcript levels of these receptors (supplemental Table S6). Many differentially expressed genes, however, were found in the cadherin family, including classic cadherin 19 (*Cdh19*) and the *Pcdhβ* cluster (*Pcdhβ2*, *Pcdhβ4*, *Pcdhβ7*, *Pcdhβ18*, and *Pcdhβ19*) as shown in Fig. 1*A* (indicated by *arrows*) and Table 2. Interestingly, all gene members of the *Pcdhβ* group were up-regulated to a different degree in *GnT-V*-null tumors (Table 2), a result validated by qRT-PCR analyses (Fig. 1, *B* and *C*). These results suggested that the protocadherin β gene cluster may function to impede tumor progression and could be involved to delay the onset of her-2-induced mammary tumors in the mice with no *GnT-V* expression (9).

To test whether the expression of *Pcdhβ* was also increased at the protein level, tumor sections were used for immunochemical staining using antibodies against *Pcdhβ4* and *Pcdhβ7* (Fig. 1*D*). Consistent with increased gene expression, *GnT-V* KO tumors in which leukocytic phytohemagglutinin binding was totally suppressed due to deletion of *GnT-V* showed increased *Pcdhβ4* and *Pcdhβ7* staining compared with wild-type tumors, indicating increased protein expression of *Pcdhβ4* and *Pcdhβ7* in *GnT-V* KO tumors.

To test whether increased expression of *Pcdhβ* genes in *GnT-V* KO tumors was indeed caused by *GnT-V* expression differences, her-2 tumor cell lines, including *GnT-V* WT cells, KO cells, and rescued KO cells (KO cells transfected with *GnT-V*), were established from tumor tissues (9), and transcript levels of *Pcdhβ2*, *Pcdhβ4*, *Pcdhβ18*, and *Pcdhβ19* were measured by qRT-PCR because these four genes showed significant -fold changes (-fold change ≥2.0, $p < 0.05$) in *GnT-V* KO tumors based on the microarray data. As show in Fig. 2*A*, increased expression of the *Pcdhβ* genes was observed in the cells derived from *GnT-V*-null tumors compared with WT tumor cells, consistent with the results obtained from microarray analyses of tumor tissues. After treatment with swainsonine, an inhibitor of *N*-linked β(1,6) branching, WT cells showed increased *Pcdhβ* gene expression (Fig. 2*B*); reintroduction of GnT-V cDNA into KO tumor cells significantly attenuated the expression of *Pcdhβ* genes in these cells (Fig. 2*C*), supporting the hypothesis that differential expression of *Pcdhβ* genes in *GnT-V* KO tumors was due to altered expression levels of GnT-V. A recent study has shown that *Pcdh* gene clusters, including the *Pcdhβ* family, are expressed at lower levels in human breast cancer tissues than in normal tissues, and these lower expression levels were linked to human breast tumorigenesis (26). To confirm and extend the observation concerning the differential expression of the *Pcdhβ* gene cluster in mouse mammary tumors after deletion of *GnT-V*, *Pcdhβ* gene expression was measured in the human breast cancer cell line MDA-MB231 after knockdown of *GnT-V* by siRNA. As shown in Fig. 2*D*, three members of the human *PCDHβ* cluster (*PCDHβ3*, *PCDHβ6*, and *PCDHβ13*), which were shown to be significantly down-regulated in human breast cancer tissues (26), were dramatically enhanced in MDA-MB231 cells with *GnT-V* knockdown, further confirming the ability of GnT-V expression levels to regulate the expression of the *Pcdhβ* cluster during breast tumorigenesis.

Differentially Expressed Pcdhβ Cluster in GnT-V KO Tumors Is Not Primarily Mediated by Altered DNA Methylation—Epigenetic aberrations are frequent events in human breast cancer development (26, 33), and promoter methylation has been

TABLE 1
Genes showing significant -fold changes by microarray analysis

Gene	Symbol	RefSeq accession no.	*p* value (KO/WT)	-Fold change (KO/WT)
Enolase 2, γ neuronal	*Eno2*	NM_013509	4.32*e*−05	−2.24011
Hedgehog-interacting protein-like 2	*Hhipl2*	BC034362	0.000242	−6.52572
Mannoside acetylglucosaminyltransferase 5	*Mgat5*	NM_145128	0.00044	−2.11392
CD14 antigen	*Cd14*	NM_009841	0.000607	2.13547
N-Acetylneuraminate pyruvate lyase	*Npl*	NM_028749	0.000753	−3.64734
—[a]		—	0.000949	−3.4074
Glucosaminyl (*N*-acetyl) transferase 1, core 2	*Gcnt1*	NM_173442	0.00149	−3.37106
—		—	0.002031	−2.03624
Regulator of G-protein signaling 2	*Rgs2*	NM_009061	0.003417	−3.81328
Adenylate kinase 3-like 1	*Ak3l1*	NM_009647	0.003423	−2.26087
RIKEN cDNA 1700040L02 gene	1700040L02Rik	BC087900	0.004049	2.81943
Interferon-activated gene 202B	*Ifi202b*	NM_008327	0.005126	−2.69043
—		—	0.009093	2.03234
Solute carrier family 38, member 3	*Slc38a3*	NM_023805	0.00921	2.13304
—		—	0.009639	2.23546
Heat shock protein 1A	*Hspa1a*	NM_010479	0.010781	−2.13604
Potassium inwardly rectifying channel, subfamily J, member 13	*Kcnj13*	NM_001110227	0.012275	−2.13735
—		—	0.01239	−2.1894
Dipeptidylpeptidase 10	*Dpp10*	NM_199021	0.01564	−4.71333
RAS guanyl-releasing protein 1	*Rasgrp1*	NM_011246	0.015876	−2.32995
ENSMUSG00000072618		ENSMUST00000100713	0.016753	3.72366
Caspase 12	*Casp12*	NM_009808	0.017624	2.50816
D-Aspartate oxidase	*Ddo*	NM_027442	0.017712	2.01305
Actin-binding LIM protein family, member 3	*Ablim3*	NM_198649	0.020009	−2.25541
Zinc finger protein 521	*Zfp521*	NM_145492	0.020746	3.12831
Protocadherin β19	*Pcdhb19*	NM_053144	0.020934	2.02627
NAD(P)H dehydrogenase, quinone 1	*Nqo1*	NM_008706	0.020957	2.4185
—		—	0.021262	2.29063
Protocadherin β18	*Pcdhb18*	NM_053143	0.021566	2.21905
—		—	0.022472	3.79211
Mohawk homeobox	*Mkx*	NM_177595	0.022573	−2.66449
V-set domain-containing T cell activation inhibitor 1	*Vtcn1*	NM_178594	0.022682	2.55331
Scrapie-responsive gene 1	*Scrg1*	NM_009136	0.023531	3.86718
—		—	0.02368	−2.07973
Major facilitator superfamily domain-containing 4	*Mfsd4*	NM_001114662	0.026284	−3.09621
Secernin 1	*Scrn1*	NM_027268	0.026819	2.32697
Insulin-like growth factor-binding protein 4	*Igfbp4*	NM_010517	0.027816	−2.30083
SPARC-related modular calcium binding 1	*Smoc1*	NM_001146217	0.027821	2.88559
Cadherin 19, type 2	*Cdh19*	NM_001081386	0.028015	−3.07028
—		—	0.028619	−2.0569
RIKEN cDNA 1700055N04 gene	1700055N04Rik	AK081788	0.03032	−2.96093
—		—	0.030372	2.20457
—		—	0.034671	−2.01378
Synaptic vesicle glycoprotein 2c	*Sv2c*	NM_029210	0.034726	−2.22967
—		—	0.036855	2.21008
—		—	0.037019	2.49757
—		—	0.037103	2.077
Protocadherin β4	*Pcdhb4*	NM_053129	0.038903	2.04059
Cytohesin 1-interacting protein	*Cytip*	NM_139200	0.039081	2.33386
TOX high mobility group box family member 3	*Tox3*	NM_172913	0.040529	−2.26008
Thrombospondin, type I, domain-containing 4	*Thsd4*	NM_001040426	0.041443	2.06645
Mucin 15	*Muc15*	NM_172979	0.043913	2.11666
Claudin 8	*Cldn8*	NM_018778	0.045599	2.66327
Protocadherin β2	*Pcdhb2*	NM_053127	0.048118	2.11683
—		—	0.048788	2.41597
Protocadherin β7	*Pcdhb7*	NM_053132	0.049552	2.15923
Low density lipoprotein receptor class A domain-containing 3	*Ldlrad3*	NM_178886	0.050311	−2.8352

[a] —, unidentified genes. *SPARC*, sereted protein, acidic, cystein-rich (osteonectin); *LIM*, lipophilic protein; *TOX*, thymocyte selection-associated high mobility group box.

implicated in the regulation of *Pcdh* clusters, including the *Pcdhβ* family (26). Also, an association between frequent CpG island methylation and *her-2* expression status was observed in human breast cancer (33, 34). To determine whether altered expression of the *Pcdhβ* cluster in *GnT-V* KO tumors was caused by promoter methylation differences, the promoter methylation status of *Pcdhβ* genes was analyzed. We first searched the mouse *Pcdhβ* cluster for CpG islands around the transcription start site (TSS) (−1 to +1 kb) using CpGPlot. As shown in supplemental Fig. 3, few CpG islands around the TSS area were found in most of the *Pcdhβ* genes (*Pcdhβ2*, *Pcdhβ4*, *Pcdhβ7*, *Pcdhβ18*, and *Pcdhβ19*) that showed alterations in

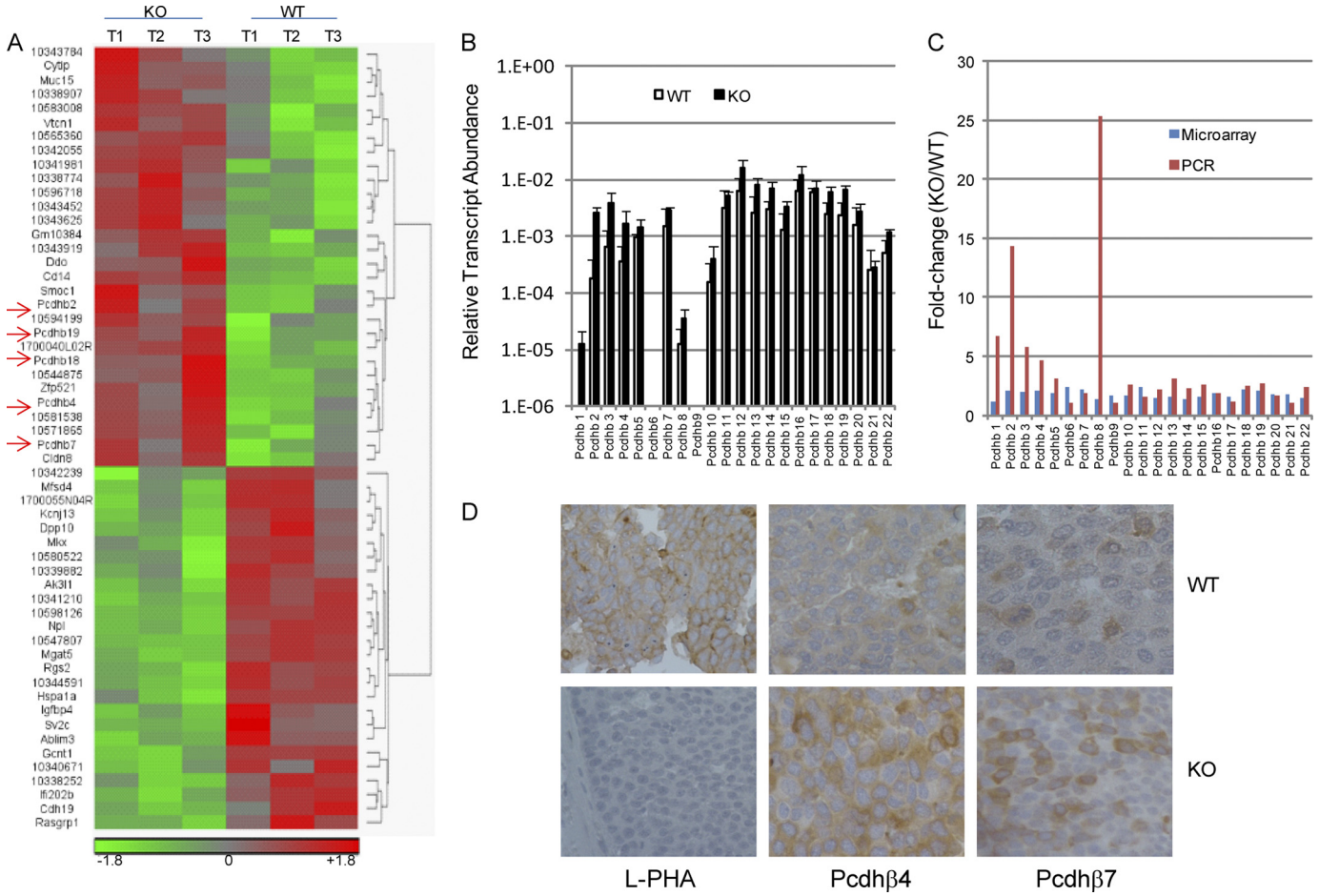

FIGURE 1. **Microarray analysis of gene expression in her-2-induced tumors.** *A*, total RNA was isolated from three wild-type and *GnT-V* knock-out tumor tissues and used for microarray analysis. A heat map of 57 transcripts differentially expressed ($p < 0.05$) between wild-type and *GnT-V* knock-out tumors was generated from the microarray data. *Red* indicates a high expression level, whereas *green* indicates a low expression level relative to wild-type. *T1–3* represents three tumor tissues collected from three mice with *GnT-V* wild-type and knock-out backgrounds, respectively. *B*, total RNA was isolated from two wild-type and two *GnT-V* knock-out tumors and used for validation of transcript levels of the *Pcdhβ* cluster by qRT-PCR. For each transcript, the values are normalized to control (*Gapdh* or *Rpl4*) and expressed as means with *error bars* indicating ±1 S.D. *C*, comparison of -fold change (KO/WT) of transcripts from microarray and qRT-PCR analyses. *D*, mammary tumor sections from 10-week-old mice were immunostained with leukocytic phytohemagglutinin (*L-PHA*), anti-Pcdhβ4, and anti-Pcdhβ7, respectively.

GnT-V-null tumors, consistent with reports that the mouse genome contains lower amounts of CpG islands than the human genome (22, 23). Interestingly, treatment of her-2 tumor cells with the demethylation drug 5-aza-2′-deoxycytidine increased expression of some *Pcdhβ* genes, such as *Pcdhβ4* and *Pcdhβ18* (Fig. 3*A*), indicating that these genes can still be regulated by methylation status regardless of the lower frequency of CpG islands. Because no CpG islands around the TSS area of *Pcdhβ4* and *Pcdhβ18* were found, it is likely that demethylation activated certain transcription activators of these genes, indirectly leading to increased gene expression. Methylation-specific PCR targeting the area surrounding the TSS was performed for the *Pcdhβ* genes that have predicted CpG island(s) around their TSS (Fig. 3*B*). Interestingly, *Cdh1*, whose gene expression is silenced due to promoter hypermethylation in many human tumors, including breast tumors (35), showed very low promoter methylation in the her-2-induced mouse mammary tumors. The same patterns of promoter methylation of *Pcdhβ* genes were observed in both wild-type and *GnT-V* KO cells, however, consistent with the unchanged expression of methylation-related genes in KO tumors observed in microarray analysis data (data not shown). These results indicated that knock-out of *GnT-V* had little effect on methylation levels of *Pcdhβ* genes. The altered gene expression of the *Pcdhβ* cluster following deletion of *GnT-V* probably does not primarily result from changes in methylation status.

Impaired Her-2-mediated Signaling Pathways Are Involved in Differentially Expressed Pcdhβ Cluster Transcripts in GnT-V KO Tumors—Deletion of *GnT-V* had no effect on *her-2* expression levels but did cause inhibition of *her-2*-induced oncogenic signaling pathways (supplemental Fig. 4) (9). Therefore, the differentially expressed *Pcdhβ* cluster in *GnT-V* KO tumors may possibly result from attenuation of her-2-induced activation of either the PKB or ERK signaling pathways. To this end, inhibitors and activators of these two signaling pathways were used to study the effect of her-2 signaling on expression of the *Pcdhβ* cluster. As shown in Fig. 4*A*, treatment of WT tumor cells with PD98059 or wortmannin, inhibitors of MAPK and PI3K/PKB signaling pathways, respectively, led to increased gene expression of the *Pcdhβ* cluster in these cells. Stimulation of KO tumor cells with EGF and neuregulin, the ligand of her-1 (EGF

TABLE 2
Microarray analyses of cadherin genes

Gene symbol	RefSeq accession no.	*p* value (KO/ WT)	-Fold change (KO/WT)
Cdh1	NM_009864	0.0482811	1.19963
Cdh10	NM_009865	0.947114	1.00215
Cdh11	NM_009866	0.0454794	−1.22638
Cdh11	NM_009866	0.190889	1.13634
Cdh12	NM_001008420	0.81751	−1.01606
Cdh13	NM_019707	0.0121108	−1.34055
Cdh15	NM_007662	0.513186	1.02147
Cdh16	NM_007663	0.221272	1.08585
Cdh17	NM_019753	0.00202595	1.09613
Cdh18	NM_001081299	0.447682	1.03206
Cdh18	NM_001081299	0.536517	−1.05179
Cdh19	NM_001081386	0.0280145	−3.07028
Cdh2	NM_007664	0.131852	−1.35843
Cdh20	NM_011800	0.560637	1.05647
Cdh22	NM_174988	0.497218	−1.02541
Cdh23	NM_023370	0.974851	1.00535
Cdh24	NM_199470	0.244223	1.04482
Cdh24	NM_199470	0.332417	1.05419
Cdh26	NM_198656	0.00252523	1.12984
Cdh3	NM_001037809	0.180038	1.39927
Cdh4	NM_009867	0.0425419	−1.0686
Cdh5	NM_009868	0.0339117	−1.50675
Cdh6	NM_007666	0.0109419	−1.05413
Cdh7	NM_172853	0.503633	1.04568
Cdh8	NM_001039154	0.0832978	−1.0873
Cdh9	NM_009869	0.616825	1.03588
Pcdhb1	NM_053126	0.0759057	1.16026
Pcdhb10	NM_053135	0.133674	1.68619
Pcdhb11	NM_053136	0.116768	2.33405
Pcdhb11	BC116321	0.918698	1.01082
Pcdhb12	NM_053137	0.208368	1.4337
Pcdhb13	NM_053138	0.404271	1.54499
Pcdhb14	NM_053139	0.266798	1.37775
Pcdhb15	NM_053140	0.155838	1.58338
Pcdhb16	NM_053141	0.0844595	1.8585
Pcdhb17	NM_053142	0.17262	1.54492
Pcdhb18	NM_053143	0.0215659	2.21905
Pcdhb19	NM_053144	0.0209341	2.02627
Pcdhb2	NM_053127	0.0481177	2.11683
Pcdhb20	NM_053145	0.0421417	1.75779
Pcdhb21	NM_053146	0.0452228	1.76552
Pcdhb22	NM_053147	0.275681	1.43601
Pcdhb3	NM_053128	0.143204	1.96662
Pcdhb4	NM_053129	0.0389026	2.04059
Pcdhb5	NM_053130	0.0149483	1.81789
Pcdhb6	NM_053131	0.0947665	2.38506
Pcdhb7	NM_053132	0.0495524	2.15923
Pcdhb8	NM_053133	0.185062	1.3181
Pcdhb9	NM_053134	0.0761935	1.66598

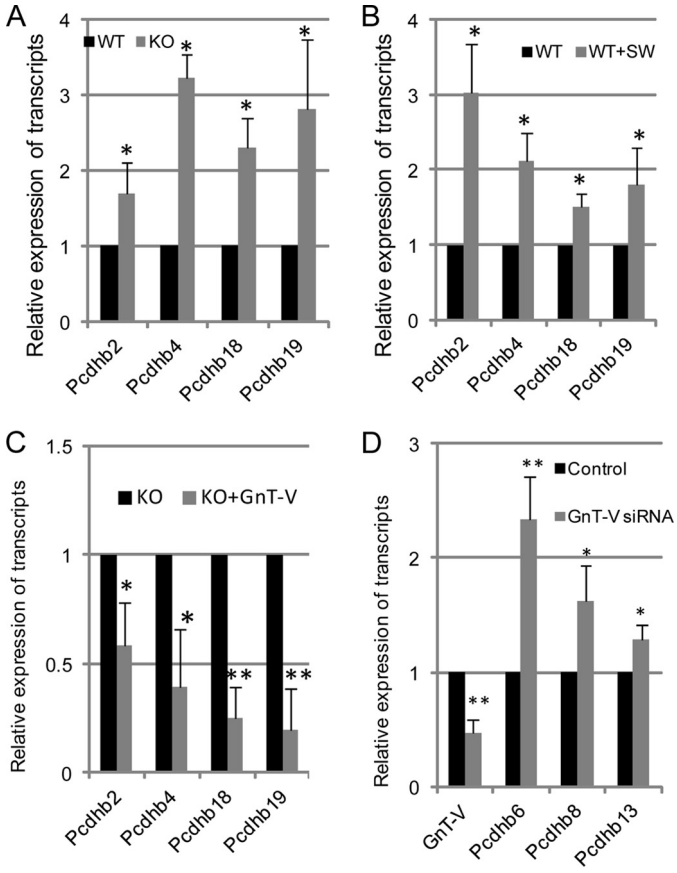

FIGURE 2. **Increased transcript expression of the *Pcdhβ* gene cluster is related to absence of GnT-V activity.** *A*, total RNA was isolated from wild-type and *GnT-V* knock-out tumor cells and used for detection of transcript levels of *Pcdhβ* genes. *B*, wild-type her-2 tumor cells were treated with swainsonine (*SW*; 1 μg/ml) for 24 h, and total RNA was isolated and used for detection of transcript levels of *Pcdhβ* by qRT-PCR. *C*, total RNA was isolated from *GnT-V* KO cells with GnT-V expression and used for detection of transcript levels of *Pcdhβ*. *D*, total RNA was isolated from control (scrambled siRNA)- and GnT-V siRNA-transfected MDA-MB231 cells and used for detection of transcript levels of *GnT-V* and *Pcdhβ* genes, respectively. For each transcript, the values are normalized to control (*Gapdh* or *Rpl4*) and expressed as means with *error bars* indicating ±1 S.D. of three independent experiments. *, Student's *t* test, $p < 0.05$; **, $p < 0.01$.

receptor) and her-3, respectively, activated her-2 signaling pathways as evident by enhanced expression levels of phospho-ERK and phospho-PKB and attenuated gene expression of *Pcdhβ* (Fig. 4*B*). These results indicated that her-2-induced signaling pathways were implicated in GnT-V-mediated gene regulation of the *Pcdhβ* cluster. To further confirm that the MAPK and PI3K/PKB pathways involved in the regulation of gene expression of *Pcdhβ* were her-2 oncoprotein-related, knockdown of *her-2* was performed using *her-2*/*neu* siRNA oligonucleotides. As shown in Fig. 4, *C–E*, a 60% reduction of her-2 in WT tumor cells treated with *her-2* siRNA was accompanied by attenuated her-2-induced downstream signaling (phospho-ERK and phospho-PKB), significantly enhancing *Pcdhβ* gene expression. This result strongly supports the conclusion that gene expression of the *Pcdhβ* cluster is regulated by her-2-induced signaling pathways. Therefore, the deletion of *GnT-V* observed in the *GnT-V*-null tumors attenuated the her-2-mediated signaling pathways, resulting in increased gene expression of the *Pcdhβ* cluster.

MiR-21 Is One of the Downstream Regulators of Her-2 Signaling Implicated in the Altered Gene Expression of Pcdhβ Cluster—Activation of her-2 signaling increases the expression of miR-21 (36, 37), which contributes to the increased invasion and metastatic potential of breast cancer cells (36). To further study whether miR-21 was involved in her-2-regulated gene expression of the *Pcdhβ* cluster, the expression of mature miR-21 and its effects on *Pcdhβ* gene expression were investigated. Consistent with inhibited her-2 signaling, approximately 75% down-regulation of miR-21 levels as detected by qRT-PCR was observed in *GnT-V*-null tumors compared with wild-type tumors (Fig. 5*A*). To verify that reduced miR-21 expression was *GnT-V*-related, we silenced *GnT-V* by siRNA expression in two human breast cancer lines, MDA-MB231 and SK-BR3, and measured miR-21 levels. We found that miR-21 expression was dramatically inhibited in both cell types after *GnT-V* knockdown as shown in Fig. 5*B*. These results demonstrated that miR-21 was regulated by expression levels of *GnT-V* in the breast cancer cells. To investigate the role of miR-21 in the

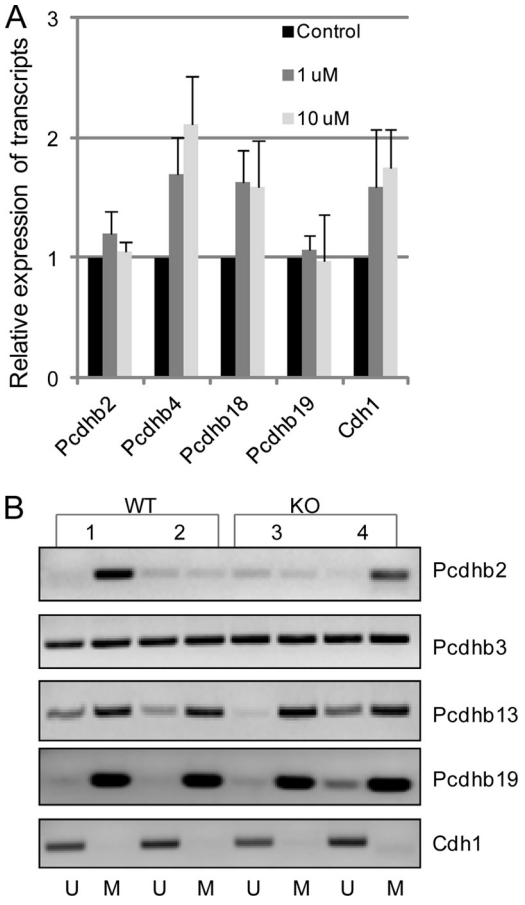

FIGURE 3. **Increased transcript expression of the *Pcdhβ* gene cluster is not primarily mediated by altered promoter methylation.** *A*, her-2 tumor cells were treated with the demethylating reagent 5-aza-2′-deoxycytidine at two different concentrations for 3 days, and total RNA was isolated and used for detection of transcript levels of *Pcdhβ*. For each transcript, the values are normalized to control (*Gapdh* or *Rpl4*) and expressed as means with *error bars* indicating ±1 S.D. of three independent experiments. *B*, after the genomic DNA samples were purified and bisulfate-treated, methylation-specific PCR for the *Pcdhβ* genes was performed in two wild-type (samples *1* and *2*) and two *GnT-V* knock-out (samples *3* and *4*) tumors. The presence of a PCR product band in *lane M* or *U* indicates methylated or unmethylated genes, respectively. Data are representative of two independent experiments.

altered gene expression of the *Pcdhβ* cluster, we transfected her-2 tumor cells (wild-type *GnT-V*) with a locked nucleic acid-modified anti-miR-21 siRNA oligonucleotide to inhibit miR-21 expression (Fig. 5*C*). Interestingly, these treatments caused to varying degrees increases in *Pcdhβ* cluster gene expression (Fig. 5*D*), indicating that the *Pcdhβ* cluster is the likely target of miR-21 because the expression of these genes was altered when miR-21 levels were reduced. Therefore, increased gene expression of the *Pcdhβ* cluster observed in *GnT-V* knock-out tumors most likely resulted at least to some extent from reduced expression of miR-21 caused by attenuated her-2 signaling. Based on computational target prediction by Targetscan, we investigated some of the predicted targets of miR-21 that either have been validated by experiments or showed significant changes by microarray analysis in our study (Table 3). From our microarray data, we identified several genes whose expression was altered, including *Rasgrp1*, *Npas3*, *Reck*, and *Epha4*, and changes in these genes were validated by qRT-PCR (data not shown). However, none of the *Pcdhβ* family members was among them, suggesting that the *Pcdhβ* gene cluster does not contain miR-21 binding sequences in their 3′-UTRs and that the altered gene expression of the *Pcdhβ* cluster in the *GnT-V*-null tumors is regulated indirectly by miR-21 expression. To further substantiate that altered expression of *Rasgrp1*, *Npas3*, *Reck*, and *Epha4* resulted from reduced miR-21 expression, the expression of these predicted miR-21 targets were determined in tumor cells whose miR-21 expression was knocked down. As shown in Fig. 5*E*, the gene expression of *Rasgrp1*, *Npas3*, *Reck*, and *Epha4* was all up-regulated after knockdown of miR-21, indicating that all genes, except for *Rasgrp1*, were indeed targets of miR-21 in the her-2 mammary tumors, which is likely responsible for the altered gene expression of the *Pcdhβ* cluster in the *GnT-V*-null tumors.

Tumor-suppressive Functions of Pcdhβ Cluster—Pcdh gene clusters have characteristics of suppressors of the transformed phenotype, and their epigenetic silencing has been implicated in some human cancer development, including breast cancer (26, 27). To determine whether the differential expression of the *Pcdhβ* cluster following deletion of *GnT-V* contributed to the delayed onset of her-2-mediated tumorigenesis, cell culture-based assays of colony formation and anchorage-independent cell growth commonly utilized for assessing tumor suppressor function were used to evaluate the ability of the *Pcdhβ* cluster to inhibit tumor progression (27). Based on the microarray data and commercial availability of clones (Source BioScience), *Pcdhβ4* and *Pcdhβ19* were chosen for these experiments. Overexpression of either *Pcdhβ4* or *Pcdhβ19* in both mouse her-2 tumor cells (wild-type) and human MDA-MB231 cells, which was confirmed by qRT-PCR and immunofluorescent staining (supplemental Fig. 5), significantly inhibited colony formation after 2 weeks compared with control cells (Fig. 6*A*). Similarly, anchorage-independent cell growth in soft agar was markedly reduced in both cell lines after transfection of *Pcdhβ4* and *Pcdhβ19* (Fig. 6*B*), indicating inhibition of cell proliferation in these cells due to the exogenous expression of *Pcdhβ* genes. To further confirm the ability of *Pcdhβ* genes to inhibit tumor progression *in vivo*, we next tested the ability of tumor cells overexpressing *Pcdhβ* to form tumors in NOD/SCID mice. Slower tumor growth was observed in xenografts resulting from injection of either her-2 tumor cells (Fig. 6, *C* and *D*) or MDA-MB231 cells (supplemental Fig. 6A), each of which was overexpressing either *Pcdhβ4* or *Pcdhβ19*, compared with mock-transfected cells. These results indicated reduced tumorigenesis due to *Pcdhβ* expression. Hematoxylin/eosin staining of tumor sections showed a reduced number of mitotic cells and less tumor necrosis in tumors resulting from injection of *Pcdhβ*-expressing cells (supplemental Fig. 6, B and C). Consistent with inhibited tumorigenesis, reduced populations of tumor-initiating cells as detected by the ALDEFLUOR assay (9) were also observed in both *Pcdhβ*-expressing her-2 tumor cells (1.47 *versus* 4.04% in control) and their xenograft tumors (2.04 *versus* 11.6% in control) in NOD/SCID mice (Fig. 6*E*). Our results are supportive of reports that *Pcdh* clusters function to suppress tumor progression and suggest that the delayed her-2-induced mammary tumor onset observed after deletion of *GnT-V* (9) might be attributed at least in part to enhanced expression of *Pcdhβ* cluster transcripts.

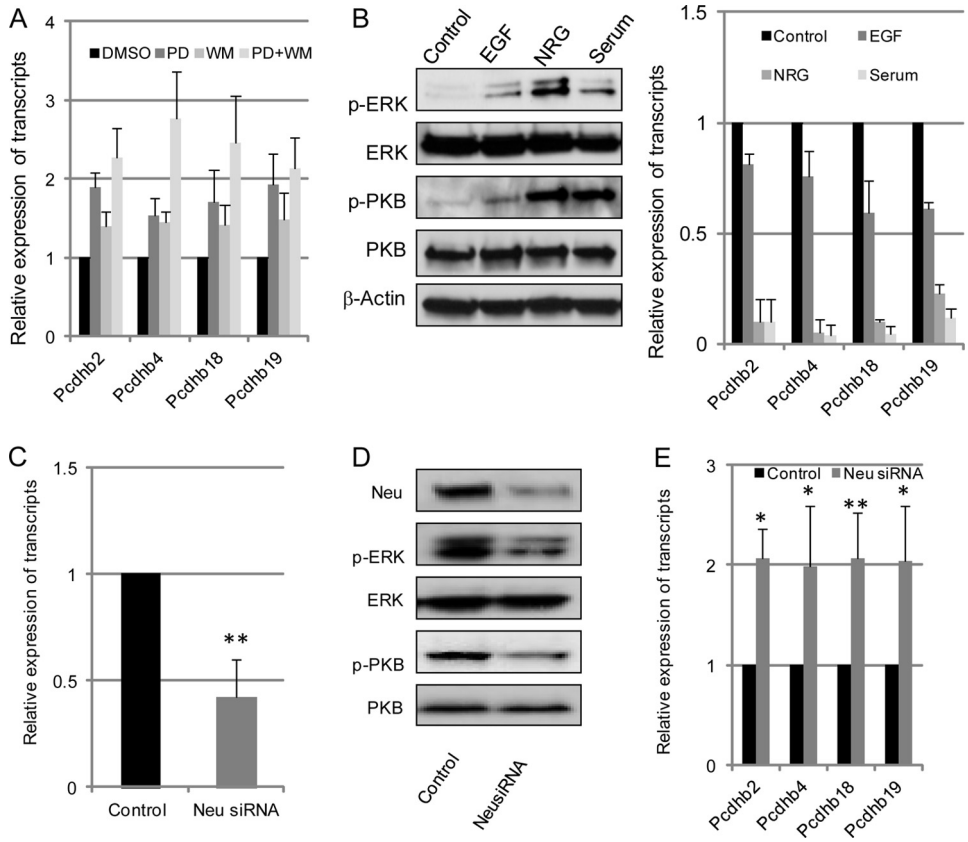

FIGURE 4. **Increased transcript expression of the *Pcdhβ* gene cluster is caused by impaired her-2-mediated downstream signaling.** *A*, wild-type tumor cells were grown for 2 days with or without MEK inhibitor PD98059 (*PD*; 10 mol/liter), PI3K inhibitor wortmannin (*WM*; 1 mol/liter), or both inhibitors. Cells were then collected, and total RNA was isolated and used for detection of transcript levels of *Pcdhβ*. *B*, *GnT-V* knock-out tumor cells were grown in serum-free medium for 2 days and stimulated with EGF (100 ng/ml), neuregulin (*NRG*) (50 ng/ml), or serum-containing medium for 2 days. Cells were collected for detection of phospho-PKB (*p-PKB*) and phospho-ERK (*p-ERK*) using immunoblot (*left panel*) and transcripts of the *Pcdhβ* cluster (*right panel*). After wild-type her-2 cells were treated with control (scrambled) and her-2/neu siRNA oligonucleotides (50 nM) for 48 h, respectively, cells were collected and subjected to detection of transcripts of her-2/neu using qRT-PCR (*C*); her-2/neu, phospho-PKB (*p-PKB*), and phospho-ERK (*p-ERK*) using immunoblot (*D*); and transcripts of the *Pcdhβ* gene cluster (*E*). For each transcript, the values are normalized to control (*Gapdh* or *Rpl4*) and expressed as means with *error bars* indicating ±1 S.D. of three independent experiments. *, Student's *t* test, $p < 0.05$; **, $p < 0.01$.

DISCUSSION

Aberrant *N*-glycosylation has been documented during tumorigenesis and tumor progression (38). We recently reported that a specific posttranslational modification by deletion of *GnT-V* disrupts mammary acinar formation and delays her-2-induced mouse mammary tumor onset by down-regulating the relative size of the compartment of tumor-initiating cells (9). In the present study, we show by microarray analysis that 142 differentially expressed genes were observed in *GnT-V* knock-out her-2-induced tumors compared with wild-type *GnT-V* her-2-induced tumors, including one group in the cadherin gene cluster, termed *Pcdhβ*, which was significantly up-regulated. Two members of this cluster were chosen and shown to suppress several characteristics of the transformed phenotype that could contribute at least in part to the reduced her-2-mediated mammary tumorigenesis observed in *GnT-V*-null mice.

Pcdh gene clusters consist of three closely linked family members designated *Pcdhα*, *Pcdhβ*, and *Pcdhγ* (22). The mouse *Pcdhβ* gene family contains 22 members (*Pcdhβ1–22*) that are organized in a tandem array on chromosome 18, and each member consists of a single exon that encodes the extracellular, transmembrane, and short cytoplasmic protein domains (22). Although *Pcdh* clusters play potential roles in neuron development (21), little is known about the cellular functions of these proteins. Unlike classic cadherins, Pcdhs appear not to function via the strong interaction of their extracellular domains as do the classic cadherins because their interactions appear to be much weaker (39, 40). Like the classic cadherins, Pcdhs are glycoproteins with *N*-linked glycan sequons located in their extracellular domains. Studies have shown that Pcdhs are proteolytically cleaved by γ-secretase complex, producing soluble intracellular fragments that may enter the nucleus and affect gene expression (41, 42). Of note, several studies have shown that the *Pcdh* superfamily may be implicated in tumor development and function as tumor suppressors. Dallosso *et al.* (27) reported that *PCDH* gene clusters, including *PCDHα*, *PCDHβ*, and *PCDHγ*, were epigenetically silenced in Wilms tumor, and ectopic expression of *PCDHγ* showed growth inhibition of tumor cells *in vitro*. Another study found that the expression of *PCDH* cluster transcripts was reduced due to promoter hypermethylation in human breast tumors compared with normal breast tissues and concluded that aberrant DNA hypermethylation of multiple *PCDH* CpG islands is a common event in human breast cancer (26). In our study, up-regulation of gene expression of the *Pcdhβ* cluster as detected by microarray anal-

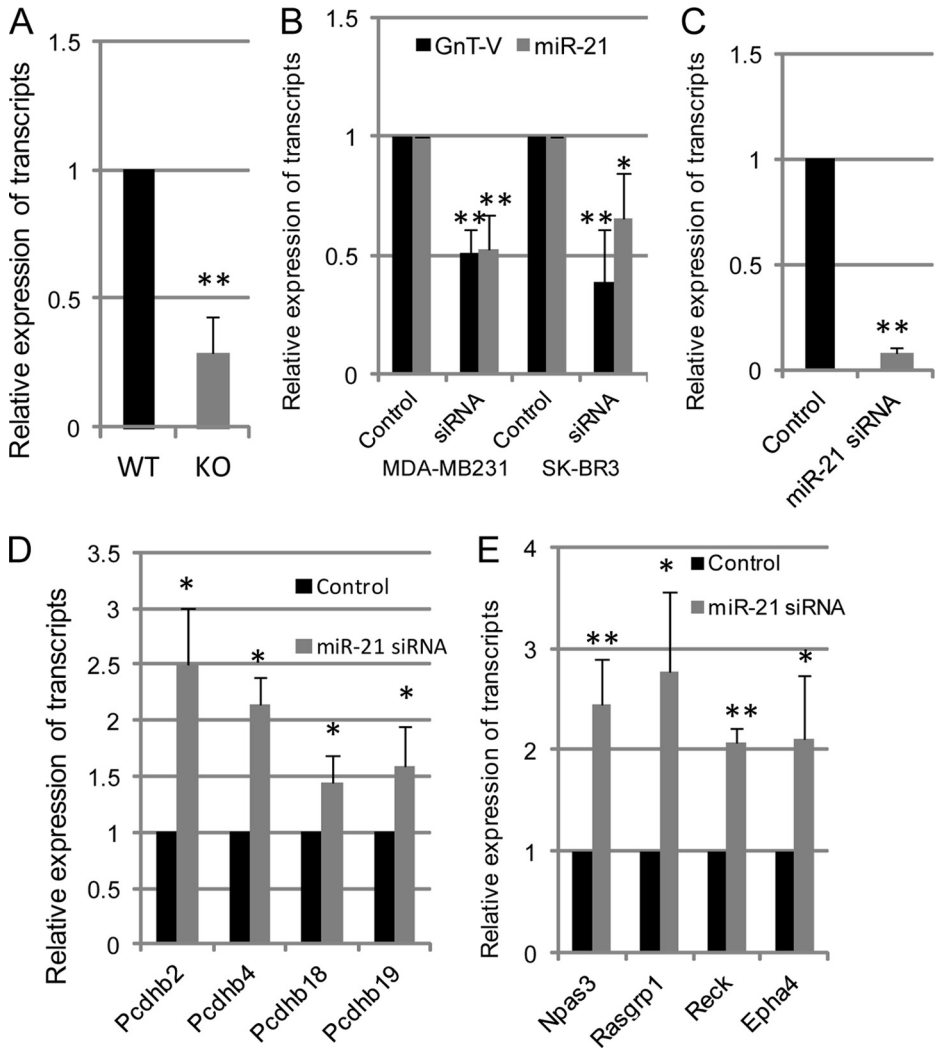

FIGURE 5. **MiR-21 is implicated in the regulation of her-2 signaling-mediated gene expression of *Pcdhβ* cluster.** *A*, total RNA was pooled from four tumors of *GnT-V* wild-type and knock-out mice, and expression of mature miR-21 was detected by qRT-PCR. *B*, total RNA was isolated from MDA-MB231 and SK-BR3 tumor cells with and without *GnT-V* siRNA expression, and expression of GnT-V and mature miR-21 was detected by qRT-PCR. After wild-type her-2 tumor cells were treated with control and anti-miR-21 siRNA oligonucleotides (50 nM) for 48 h, respectively, cells were collected and subjected to detection for transcripts of miR-21 (*C*), the *Pcdhβ* cluster (*D*), and miR-21 target genes as indicated (*E*). For each transcript, the values are normalized to control (*Gapdh* or *Rpl4*) and expressed as means with *error bars* indicating ±1 S.D. of three independent experiments. *, Student's *t* test, $p < 0.05$; **, $p < 0.01$.

TABLE 3
MiR-21 target genes based on Targetscan

Gene symbol	*p* value	-Fold change (KO/WT)
Jag1	0.065	−1.3
Rasgrp1	0.02	−2.3
Sox2	0.032	−1.37
Npas3	0.002	1.87
Btg2	0.032	−1.29
Reck	0.087	1.45
Sox7	0.0008	−1.26
Epha4	0.004	1.55
Nfat5	0.025	1.31
Pdcd4	0.25	−1.14
Tgfb1	0.14	−1.46
Nfib	0.029	1.09
Bcl2	0.71	−1.02
Pten	0.69	−1.01
Spry2	0.9	1.01
Tpm1	0.15	1.29

yses was observed in her-2-mediated breast tumors with *GnT-V* deletion compared with *GnT-V* wild-type tumors. These changes were further confirmed by qRT-PCR and proved to be *GnT-V*-related by both rescue experiments in which *GnT-V* cDNA was reintroduced into *GnT-V* knock-out tumor cells and inhibition experiments in which swainsonine was used to inhibit the biosynthesis of *N*-linked β(1,6) branching in *GnT-V* wild-type cells. Supporting these results, a human breast cancer cell line, MDA-MB231, also showed increased gene expression of some *Pcdhβ* family members after inhibition of *GnT-V* in these cells by *GnT-V* siRNA expression. These results indicate that expression levels of *GnT-V* regulate gene expression of the *Pcdhβ* cluster in mammary tumor tissues and cells, and the altered gene expression of *Pcdhβ* is implicated in the attenuation of her-2-induced tumorigenesis caused by deletion of *GnT-V* (9).

To further understand the role of altered gene expression of *Pcdhβ* cluster in the inhibition of her-2-induced tumor development that we observed previously, we subcloned two family members of the *Pcdhβ* cluster, *Pcdhβ4* and *Pcdhβ19*, into an expression vector and stably transfected mouse and human breast cancer cells. Results obtained from these experiments strongly suggest that *Pcdhβ* genes display some features of

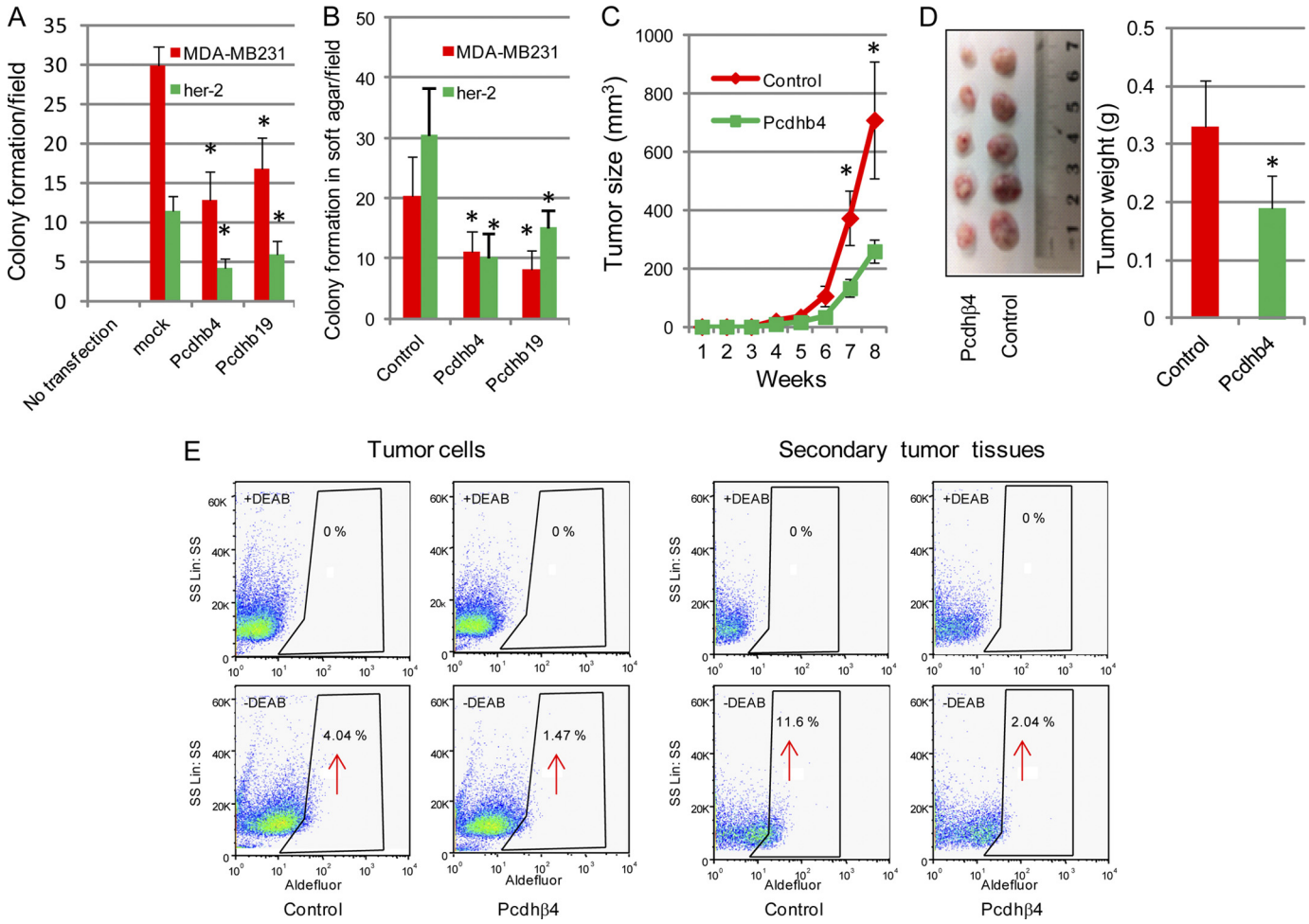

FIGURE 6. **Tumor-suppressive effects of the Pcdhβ cluster.** *A*, wild-type her-2 tumor cells and MDA-MB231 cells were transfected with either *Pcdhβ4* or *Pcdhβ19* cDNA and grown in selection medium for 2–3 weeks for colony formation. The number of colonies in six random fields was counted and expressed as the mean with *error bars* indicating ±1 S.D. * represents Student's *t* test, $p < 0.001$. *B*, transfected cells were grown in soft agar for 2–3 weeks, and the number of colonies in six random fields was counted and expressed as the mean with *error bars* indicating ±1 S.D. *, $p < 0.05$. *C*, Pcdhβ4-transfected wild-type her-2 tumor cells (2×10^6) were injected into mammary fat pads of SCID mice ($n = 5$), and secondary tumor growth was observed for up to 8 weeks. *, $p < 0.05$. *D*, secondary tumors in SCID mice formed by injection of Pcdhβ4-expressing cells were dissected at week 8 and photographed (*left panel*), and the weight of tumors was quantified and expressed as the mean with *error bars* indicating ±1 S.D. ($n = 5$; *right panel*). *, $p < 0.05$. *E*, ALDEFLUOR assays of *Pcdhβ4*-expressing her-2 tumor cells (*left panel*) and xenografts formed by injection of *Pcdhβ4*-expressing her-2 cells (*right panel*) were performed, and the percentage of ALDEFLUOR-positive cells (tumor initiating cells) was determined using similar gating criteria. Data are representative of two independent experiments. *DEAB*, diethylaminobenzaldehyde.

genes that suppress or inhibit tumor progression. First, anchorage-independent cell growth in soft agar and colony formation ability after transfection, two commonly used methods to evaluate tumor suppressor function, were remarkably inhibited when *Pcdhβ* was expressed in both mouse and human breast cancer lines. Second, *in vivo* tumor growth in NOD/SCID mice that resulted from injection of tumor cells expressing *Pcdhβ* was significantly suppressed compared with that observed from injection of control mock-transfected cells. Third, a reduced proportion of tumor-initiating cells was observed in tumor cells with *Pcdhβ* expression, consistent with the inhibited tumor growth of these cells injected in NOD/SCID mice. Based on these observations, it is reasonable to conclude that *Pcdhβ* expression may function to inhibit some aspects of the transformed phenotype. The decreased tumorigenesis and the observed inhibition of her-2-induced breast tumor onset associated with *GnT-V* deletion (9), therefore, can be attributed at least in part to the increased gene expression of the *Pcdhβ* cluster.

Aberrant levels and patterns of DNA methylation have been found as ubiquitous events in many human cancers (43). Hypermethylation of promoter CpG islands, frequently observed in human breast cancer, is related to transcriptional silencing of some genes, including tumor suppressor genes (44). Although studies have shown that gene expression of *PCDH* clusters was epigenetically regulated through changes in promoter methylation patterns in some human cancers (26, 27, 33), the altered expression of the *Pcdhβ* cluster caused by *GnT-V* deletion in our study appeared not to result from aberrant DNA methylation of *Pcdhβ* genes. Despite the fact that fewer CpG islands are predicted in promoter areas of mouse *Pcdh* gene clusters compared with human *PCDH* clusters (22, 23), higher DNA methylation levels as detected by methylation-specific PCR were still observed in her-2 tumors or cells derived

from these tumors after treatment with a methylation inhibitor, consistent with the previous observation that DNA methylation levels are increased in her-2-positive primary breast cancers (33). However, deletion of *GnT-V* had little effect on the DNA methylation status of *Pcdhβ* genes because the same patterns of methylation in *GnT-V* knock-out tumors were observed as those in wild-type tumors. These results indicated that DNA methylation of the *Pcdhβ* cluster was not regulated by GnT-V expression levels, and altered gene expression of the *Pcdhβ* cluster caused by null *GnT-V* was not likely due to the changes in DNA methylation. Supporting this conclusion, no significant changes in expression of DNA methylation-related enzymes, such as DNMT1, DNMT3A, and DNMT3B, were observed in the comparison of *GnT-V* knock-out and wild-type tumors by microarray analyses.

Although results from microarray analyses showed that deletion of *GnT-V* had little effect on expression of her-2 and other oncoproteins from the EGF family, such as her-3 and EGF receptor (her-1), consistent with our previous results (9), we found that two major downstream signaling pathways mediated by her-2 activation, the ERK and PI3K/PKB pathways, are significantly inhibited in *GnT-V* knock-out tumors (9). This result prompted us to investigate further whether aberrant her-2-mediated signaling pathways were implicated in altered gene expression of the *Pcdhβ* cluster observed in *GnT-V* knock-out tumors. We observed that stimulation of *GnT-V* knock-out cells with growth factors (EGF and neuregulin) significantly inhibited gene expression of the *Pcdhβ* cluster, whereas treatment of *GnT-V* wild-type tumor cells with PD98059 and wortmannin, inhibitors of ERK and PKB, respectively, remarkably enhanced gene expression of the *Pcdhβ* family, indicating the direct involvement of these two pathways in regulating *Pcdhβ* gene expression. The regulation of her-2-mediated signaling pathways on the gene expression of the *Pcdhβ* cluster was further confirmed by silencing her-2 oncoprotein by *her-2* siRNA expression, demonstrating that altered gene expression of the *Pcdhβ* family closely followed changes in her-2 expression levels. These results strongly argue that her-2-mediated downstream signaling pathways negatively regulated the expression of the *Pcdhβ* cluster. Deletion of *GnT-V* impaired her-2 signaling pathways, therefore attenuating the inhibition of her-2 signaling on the gene expression of the *Pcdhβ* family. The involvement of other signaling pathways in regulating gene expression of the *Pcdhβ* family in *GnT-V* knock-out tumors cannot be ruled out, however, because of the ability of GnT-V glycan products to modify the function of other glycoprotein receptors.

To further investigate the mechanisms governing how impaired her-2-mediated downstream signaling positively regulates gene expression of the *Pcdhβ* cluster in *GnT-V*-null tumors, we explored the possible downstream effectors that are regulated by her-2-mediated signaling pathways that could be involved in the regulation of *Pcdhβ* cluster expression in *GnT-V*-null tumors. MicroRNAs constitute an abundant class of non-coding RNAs of about 21–23 nucleotides that negatively regulate protein expression by targeting mRNA transcripts and mediate either translational repression or degradation of targeted mRNA (45, 46). There is increasing evidence that microRNAs are key molecules involved in cancer initiation and progression (47, 48). Functioning as an oncogene (49), miR-21 is one of the most studied microRNAs associated with cancer and is highly up-regulated in breast cancer (50, 51). Studies have shown that her-2 signaling activates several transcription factors, such as Ets-1 and Ap-1, that stimulate the expression of miR-21 (36, 37), and increased metastatic potential of her-2-expressing breast cancer cells is mediated by up-regulation of miR-21 (36). Altered expression of miR-21 may, therefore, be one of the downstream regulators of her-2 signaling implicated in her-2-mediated up-regulation of the *Pcdhβ* cluster. Consistent with impaired her-2 signaling pathways, the expression of miR-21 was significantly reduced in *GnT-V* knock-out tumors. Mostly importantly, silencing of miR-21 using a locked nucleic acid-modified anti-miR-21 resulted in the enhancement to different degrees of the expression of the *Pcdhβ* gene cluster, indicating the involvement of miR-21 in the altered gene expression of *Pcdhβ* caused by inhibited her-2 signaling at least in part. Interestingly, the effect of regulation of miR-21 on *Pcdhβ* expression appeared to be indirect because *Pcdhβ* genes are not among the predicted potential targets of miR-21 due to the lack of binding sequences for miR-21 in their 3′-UTRs. Although some of the miR-21 target genes that have been experimentally confirmed were not affected by reduced miR-21 expression in our study, including *Pdcd4*, *Pten*, *Tpm1*, and *Spry2* (49), effects on the expression of other target genes, for example *Npas3*, a newly confirmed tumor suppressor gene (52); *Reck*, a membrane-associated inhibitor of metalloproteinases and recently confirmed miR-21 target gene (53); and *Epha4*, a member of the Eph receptor tyrosine kinases (54), were observed. These targets were further validated by miR-21 silencing experiments (Fig. 5*E*) and likely mediate miR-21 regulation of the expression of the *Pcdhβ* gene cluster. Indirect regulation of genes by miR-21 has been documented; for example, an array expression analysis of MCF-7 cells depleted of miR-21 by siRNA identified miR-21 target genes that were subsequently experimentally validated, including targets that did not contain miR-21 binding sequences in their 3′-UTRs (55). Also, miR-21 was found to indirectly inhibit the expression of DNMT1 by targeting *Rasgrp1*, a critical upstream regulator of the Ras-MAPK signaling cascade, which modulates DNMT1 levels in lupus $CD4^+$ T cells (56). Another indirect regulation of *Bcl-2* by miR-21 has also been reported in breast cancer (57).

The attenuation of her-2-mediated signaling pathways observed in *GnT-V* KO tumor cells is likely to be the result of aberrant *N*-glycosylation of her-2 and/or the ErbB family of receptors that can lead to altered ligand (EGF and neuregulin) binding, regulation of the endocytosis of signaling complexes, and/or inhibition of dimer and multimer formation among members of this family (13, 58, 59). Experiments are in progress to determine the mechanisms by which β(1,6) *N*-linked glycosylation regulates her-2 function.

In conclusion, we provide evidence that a gene cluster in the cadherin superfamily, *Pcdhβ*, functions to inhibit her-2-mediated mouse mammary tumorigenicity. Our results show that *GnT-V* expression levels regulate the expression of members of the *Pcdhβ* cluster by affecting her-2-mediated downstream signaling pathways. This increased *Pcdhβ* expression is mediated

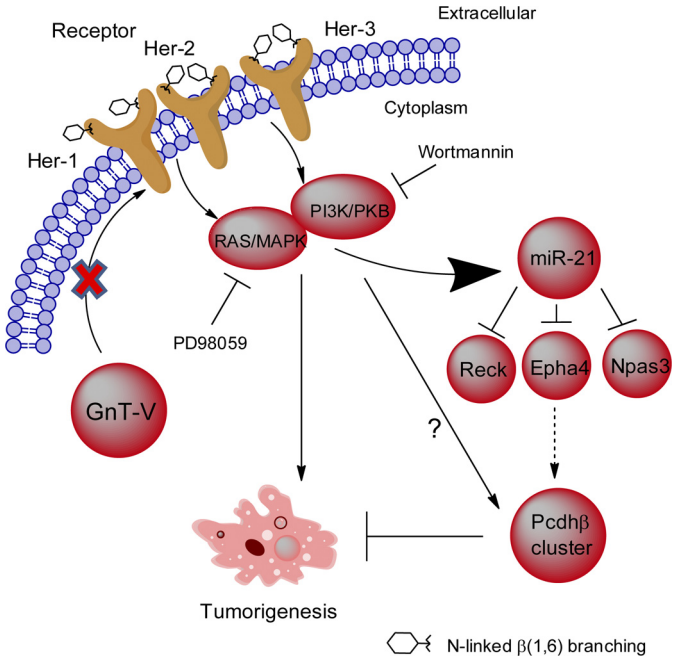

FIGURE 7. **Schematic indicating how the expression of the *Pcdhβ* gene cluster is regulated by GnT-V.** Pathways implicated in the regulation of the *Pcdhβ* gene cluster are depicted based on the observations presented in this study. GnT-V expression levels regulate *N*-glycosylation of her-2 and her-2-induced signaling pathways. Knock-out of *GnT-V* results in inhibited expression of *N*-linked β(1,6) branching on her-2 and impaired her-2-induced signaling pathways, which leads to up-regulation of the *Pcdhβ* gene cluster. The increased *Pcdhβ* expression is mediated indirectly at least in part by miR-21, one of the downstream effectors regulated by her-2 signaling, and contributes to the inhibition of her-2-induced tumor onset.

at least in part by miR-21, one of the downstream effectors regulated by her-2 signaling (Fig. 7). Because up to 30% of human breast tumors are her-2-positive (15, 16), our findings shed new light on the molecular mechanisms of the suppressive effects of *GnT-V* deletion on mammary tumorigenesis and progression and illuminate GnT-V as a potential target for an inhibitor with therapeutic utility for her-2-positive human breast cancer.

Acknowledgments—We thank the Cancer Research Center-Integrated Genomics Core at the Georgia Health Sciences University, Nikki Harvel, and Dr. Lesleyann Hawthorn for kind help with microarray analysis and Drs. Jin-kyu Lee, Karen Abbott, Hong Qiu, and Bing Zhang for informative discussions.

REFERENCES

1. Boscher, C., Dennis, J. W., and Nabi, I. R. (2011) Glycosylation, galectins and cellular signaling. *Curr. Opin. Cell Biol.* **23,** 383–392
2. Hakomori, S. (2002) Glycosylation defining cancer malignancy: new wine in an old bottle. *Proc. Natl. Acad. Sci. U.S.A.* **99,** 10231–10233
3. Zhao, Y. Y., Takahashi, M., Gu, J. G., Miyoshi, E., Matsumoto, A., Kitazume, S., and Taniguchi, N. (2008) Functional roles of *N*-glycans in cell signaling and cell adhesion in cancer. *Cancer Sci.* **99,** 1304–1310
4. Demetriou, M., Nabi, I. R., Coppolino, M., Dedhar, S., and Dennis, J. W. (1995) Reduced contact-inhibition and substratum adhesion in epithelial cells expressing GlcNAc-transferase V. *J. Cell Biol.* **130,** 383–392
5. Granovsky, M., Fata, J., Pawling, J., Muller, W. J., Khokha, R., and Dennis, J. W. (2000) Suppression of tumor growth and metastasis in Mgat5-deficient mice. *Nat. Med.* **6,** 306–312
6. Guo, H. B., Lee, I., Kamar, M., Akiyama, S. K., and Pierce, M. (2002) Aberrant *N*-glycosylation of β1 integrin causes reduced α5β1 integrin clustering and stimulates cell migration. *Cancer Res.* **62,** 6837–6845
7. Handerson, T., Camp, R., Harigopal, M., Rimm, D., and Pawelek, J. (2005) β1,6-Branched oligosaccharides are increased in lymph node metastases and predict poor outcome in breast carcinoma. *Clin. Cancer Res.* **11,** 2969–2973
8. Yamamoto, H., Swoger, J., Greene, S., Saito, T., Hurh, J., Sweeley, C., Leestma, J., Mkrdichian, E., Cerullo, L., Nishikawa, A., Ihara, Y., Taniguchi, N., and Moskal, J. R. (2000) β1,6-*N*-Acetylglucosamine-bearing *N*-glycans in human gliomas: implications for a role in regulating invasivity. *Cancer Res.* **60,** 134–142
9. Guo, H. B., Johnson, H., Randolph, M., Nagy, T., Blalock, R., and Pierce, M. (2010) Specific posttranslational modification regulates early events in mammary carcinoma formation. *Proc. Natl. Acad. Sci. U.S.A.* **107,** 21116–21121
10. Seelentag, W. K., Li, W. P., Schmitz, S. F., Metzger, U., Aeberhard, P., Heitz, P. U., and Roth, J. (1998) Prognostic value of β1,6-branched oligosaccharides in human colorectal carcinoma. *Cancer Res.* **58,** 5559–5564
11. Guo, H. B., Johnson, H., Randolph, M., and Pierce, M. (2009) Regulation of homotypic cell-cell adhesion by branched *N*-glycosylation of N-cadherin extracellular EC2 and EC3 domains. *J. Biol. Chem.* **284,** 34986–34997
12. Pinho, S. S., Reis, C. A., Paredes, J., Magalhães, A. M., Ferreira, A. C., Figueiredo, J., Xiaogang, W., Carneiro, F., Gärtner, F., and Seruca, R. (2009) The role of *N*-acetylglucosaminyltransferase III and V in the post-transcriptional modifications of E-cadherin. *Hum. Mol. Genet.* **18,** 2599–2608
13. Partridge, E. A., Le Roy, C., Di Guglielmo, G. M., Pawling, J., Cheung, P., Granovsky, M., Nabi, I. R., Wrana, J. L., and Dennis, J. W. (2004) Regulation of cytokine receptors by Golgi *N*-glycan processing and endocytosis. *Science* **306,** 120–124
14. Guo, H. B., Randolph, M., and Pierce, M. (2007) Inhibition of a specific *N*-glycosylation activity results in attenuation of breast carcinoma cell invasiveness-related phenotypes: inhibition of epidermal growth factor-induced dephosphorylation of focal adhesion kinase. *J. Biol. Chem.* **282,** 22150–22162
15. Carlsson, J., Nordgren, H., Sjöström, J., Wester, K., Villman, K., Bengtsson, N. O., Ostenstad, B., Lundqvist, H., and Blomqvist, C. (2004) HER2 expression in breast cancer primary tumours and corresponding metastases. Original data and literature review. *Br. J. Cancer* **90,** 2344–2348
16. Slamon, D. J., Clark, G. M., Wong, S. G., Levin, W. J., Ullrich, A., and McGuire, W. L. (1987) Human breast cancer: correlation of relapse and survival with amplification of the HER-2/neu oncogene. *Science* **235,** 177–182
17. Muller, W. J., Sinn, E., Pattengale, P. K., Wallace, R., and Leder, P. (1988) Single-step induction of mammary adenocarcinoma in transgenic mice bearing the activated c-neu oncogene. *Cell* **54,** 105–115
18. Guy, C. T., Webster, M. A., Schaller, M., Parsons, T. J., Cardiff, R. D., and Muller, W. J. (1992) Expression of the neu protooncogene in the mammary epithelium of transgenic mice induces metastatic disease. *Proc. Natl. Acad. Sci. U.S.A.* **89,** 10578–10582
19. Takeichi, M. (1995) Morphogenetic roles of classic cadherins. *Curr. Opin. Cell Biol.* **7,** 619–627
20. Yagi, T., and Takeichi, M. (2000) Cadherin superfamily genes: functions, genomic organization, and neurologic diversity. *Genes Dev.* **14,** 1169–1180
21. Morishita, H., and Yagi, T. (2007) Protocadherin family: diversity, structure, and function. *Curr. Opin. Cell Biol.* **19,** 584–592
22. Wu, Q., and Maniatis, T. (1999) A striking organization of a large family of human neural cadherin-like cell adhesion genes. *Cell* **97,** 779–790
23. Wu, Q., Zhang, T., Cheng, J. F., Kim, Y., Grimwood, J., Schmutz, J., Dickson, M., Noonan, J. P., Zhang, M. Q., Myers, R. M., and Maniatis, T. (2001) Comparative DNA sequence analysis of mouse and human protocadherin gene clusters. *Genome Res.* **11,** 389–404
24. Wu, Q., and Maniatis, T. (2000) Large exons encoding multiple ectodomains are a characteristic feature of protocadherin genes. *Proc. Natl. Acad. Sci. U.S.A.* **97,** 3124–3129
25. Yu, J. S., Koujak, S., Nagase, S., Li, C. M., Su, T., Wang, X., Keniry, M., Memeo, L., Rojtman, A., Mansukhani, M., Hibshoosh, H., Tycko, B., and

Parsons, R. (2008) PCDH8, the human homolog of PAPC, is a candidate tumor suppressor of breast cancer. *Oncogene* **27,** 4657–4665
26. Novak, P., Jensen, T., Oshiro, M. M., Watts, G. S., Kim, C. J., and Futscher, B. W. (2008) Agglomerative epigenetic aberrations are a common event in human breast cancer. *Cancer Res.* **68,** 8616–8625
27. Dallosso, A. R., Hancock, A. L., Szemes, M., Moorwood, K., Chilukamarri, L., Tsai, H. H., Sarkar, A., Barasch, J., Vuononvirta, R., Jones, C., Pritchard-Jones, K., Royer-Pokora, B., Lee, S. B., Owen, C., Malik, S., Feng, Y., Frank, M., Ward, A., Brown, K. W., and Malik, K. (2009) Frequent long-range epigenetic silencing of protocadherin gene clusters on chromosome 5q31 in Wilms' tumor. *PLoS Genet.* **5,** e1000745
28. Yu, J., Cheng, Y. Y., Tao, Q., Cheung, K. F., Lam, C. N., Geng, H., Tian, L. W., Wong, Y. P., Tong, J. H., Ying, J. M., Jin, H., To, K. F., Chan, F. K., and Sung, J. J. (2009) Methylation of protocadherin 10, a novel tumor suppressor, is associated with poor prognosis in patients with gastric cancer. *Gastroenterology* **136,** 640–651.e1
29. Nairn, A. V., Kinoshita-Toyoda, A., Toyoda, H., Xie, J., Harris, K., Dalton, S., Kulik, M., Pierce, J. M., Toida, T., Moremen, K. W., and Linhardt, R. J. (2007) Glycomics of proteoglycan biosynthesis in murine embryonic stem cell differentiation. *J. Proteome Res.* **6,** 4374–4387
30. Sharbati-Tehrani, S., Kutz-Lohroff, B., Bergbauer, R., Scholven, J., and Einspanier, R. (2008) miR-Q: a novel quantitative RT-PCR approach for the expression profiling of small RNA molecules such as miRNAs in a complex sample. *BMC Mol. Biol.* **9,** 34
31. Gürlevik, E., Woller, N., Schache, P., Malek, N. P., Wirth, T. C., Zender, L., Manns, M. P., Kubicka, S., and Kühnel, F. (2009) p53-dependent antiviral RNA-interference facilitates tumor-selective viral replication. *Nucleic Acids Res.* **37,** e84
32. Ginestier, C., Hur, M. H., Charafe-Jauffret, E., Monville, F., Dutcher, J., Brown, M., Jacquemier, J., Viens, P., Kleer, C. G., Liu, S., Schott, A., Hayes, D., Birnbaum, D., Wicha, M. S., and Dontu, G. (2007) ALDH1 is a marker of normal and malignant human mammary stem cells and a predictor of poor clinical outcome. *Cell Stem Cell* **1,** 555–567
33. Fiegl, H., Millinger, S., Goebel, G., Müller-Holzner, E., Marth, C., Laird, P. W., and Widschwendter, M. (2006) Breast cancer DNA methylation profiles in cancer cells and tumor stroma: association with HER-2/neu status in primary breast cancer. *Cancer Res.* **66,** 29–33
34. Terada, K., Okochi-Takada, E., Akashi-Tanaka, S., Miyamoto, K., Taniyama, K., Tsuda, H., Asada, K., Kaminishi, M., and Ushijima, T. (2009) Association between frequent CpG island methylation and HER2 amplification in human breast cancers. *Carcinogenesis* **30,** 466–471
35. Hoque, M. O., Prencipe, M., Poeta, M. L., Barbano, R., Valori, V. M., Copetti, M., Gallo, A. P., Brait, M., Maiello, E., Apicella, A., Rossiello, R., Zito, F., Stefania, T., Paradiso, A., Carella, M., Dallapiccola, B., Murgo, R., Carosi, I., Bisceglia, M., Fazio, V. M., Sidransky, D., and Parrella, P. (2009) Changes in CpG islands promoter methylation patterns during ductal breast carcinoma progression. *Cancer Epidemiol. Biomarkers Prev.* **18,** 2694–2700
36. Huang, T. H., Wu, F., Loeb, G. B., Hsu, R., Heidersbach, A., Brincat, A., Horiuchi, D., Lebbink, R. J., Mo, Y. Y., Goga, A., and McManus, M. T. (2009) Up-regulation of miR-21 by HER2/neu signaling promotes cell invasion. *J. Biol. Chem.* **284,** 18515–18524
37. Fujita, S., Ito, T., Mizutani, T., Minoguchi, S., Yamamichi, N., Sakurai, K., and Iba, H. (2008) miR-21 gene expression triggered by AP-1 is sustained through a double-negative feedback mechanism. *J. Mol. Biol.* **378,** 492–504
38. Pierce, J. M. (2009) in *Handbook of Glycomics* (Cummings, R. D., and Pierce, J. M., eds) 1st Ed., pp. 399–429, Elsevier, London
39. Obata, S., Sago, H., Mori, N., Rochelle, J. M., Seldin, M. F., Davidson, M., St John, T., Taketani, S., and Suzuki, S. T. (1995) Protocadherin Pcdh2 shows properties similar to, but distinct from, those of classical cadherins. *J. Cell Sci.* **108,** 3765–3773
40. Morishita, H., Umitsu, M., Murata, Y., Shibata, N., Udaka, K., Higuchi, Y., Akutsu, H., Yamaguchi, T., Yagi, T., and Ikegami, T. (2006) Structure of the cadherin-related neuronal receptor/protocadherin-α first extracellular cadherin domain reveals diversity across cadherin families. *J. Biol. Chem.* **281,** 33650–33663
41. Hambsch, B., Grinevich, V., Seeburg, P. H., and Schwarz, M. K. (2005) γ-Protocadherins, presenilin-mediated release of C-terminal fragment promotes locus expression. *J. Biol. Chem.* **280,** 15888–15897
42. Buchanan, S. M., Schalm, S. S., and Maniatis, T. (2010) Proteolytic processing of protocadherin proteins requires endocytosis. *Proc. Natl. Acad. Sci. U.S.A.* **107,** 17774–17779
43. Jones, P. A., and Baylin, S. B. (2007) The epigenomics of cancer. *Cell* **128,** 683–692
44. Widschwendter, M., and Jones, P. A. (2002) DNA methylation and breast carcinogenesis. *Oncogene* **21,** 5462–5482
45. Wu, L., Fan, J., and Belasco, J. G. (2006) MicroRNAs direct rapid deadenylation of mRNA. *Proc. Natl. Acad. Sci. U.S.A.* **103,** 4034–4039
46. Eulalio, A., Huntzinger, E., and Izaurralde, E. (2008) Getting to the root of miRNA-mediated gene silencing. *Cell* **132,** 9–14
47. Lu, J., Getz, G., Miska, E. A., Alvarez-Saavedra, E., Lamb, J., Peck, D., Sweet-Cordero, A., Ebert, B. L., Mak, R. H., Ferrando, A. A., Downing, J. R., Jacks, T., Horvitz, H. R., and Golub, T. R. (2005) MicroRNA expression profiles classify human cancers. *Nature* **435,** 834–838
48. Calin, G. A., and Croce, C. M. (2006) MicroRNA signatures in human cancers. *Nat. Rev. Cancer* **6,** 857–866
49. Selcuklu, S. D., Donoghue, M. T., and Spillane, C. (2009) miR-21 as a key regulator of oncogenic processes. *Biochem. Soc. Trans.* **37,** 918–925
50. Volinia, S., Calin, G. A., Liu, C. G., Ambs, S., Cimmino, A., Petrocca, F., Visone, R., Iorio, M., Roldo, C., Ferracin, M., Prueitt, R. L., Yanaihara, N., Lanza, G., Scarpa, A., Vecchione, A., Negrini, M., Harris, C. C., and Croce, C. M. (2006) A microRNA expression signature of human solid tumors defines cancer gene targets. *Proc. Natl. Acad. Sci. U.S.A.* **103,** 2257–2261
51. Si, M. L., Zhu, S., Wu, H., Lu, Z., Wu, F., and Mo, Y. Y. (2007) miR-21-mediated tumor growth. *Oncogene* **26,** 2799–2803
52. Moreira, F., Kiehl, T. R., So, K., Ajeawung, N. F., Honculada, C., Gould, P., Pieper, R. O., and Kamnasaran, D. (2011) NPAS3 demonstrates features of a tumor suppressive role in driving the progression of astrocytomas. *Am. J. Pathol.* **179,** 462–476
53. Hayashi, T., Koyama, N., Azuma, Y., and Kashimata, M. (2011) Mesenchymal miR-21 regulates branching morphogenesis in murine submandibular gland *in vitro*. *Dev. Biol.* **352,** 299–307
54. Pasquale, E. B. (2010) Eph receptors and ephrins in cancer: bidirectional signalling and beyond. *Nat. Rev. Cancer* **10,** 165–180
55. Frankel, L. B., Christoffersen, N. R., Jacobsen, A., Lindow, M., Krogh, A., and Lund, A. H. (2008) Programmed cell death 4 (PDCD4) is an important functional target of the microRNA miR-21 in breast cancer cells. *J. Biol. Chem.* **283,** 1026–1033
56. Pan, W., Zhu, S., Yuan, M., Cui, H., Wang, L., Luo, X., Li, J., Zhou, H., Tang, Y., and Shen, N. (2010) MicroRNA-21 and microRNA-148a contribute to DNA hypomethylation in lupus $CD4^+$ T cells by directly and indirectly targeting DNA methyltransferase 1. *J. Immunol.* **184,** 6773–6781
57. Adams, B. D., Furneaux, H., and White, B. A. (2007) The micro-ribonucleic acid (miRNA) miR-206 targets the human estrogen receptor-α (ERα) and represses ERα messenger RNA and protein expression in breast cancer cell lines. *Mol. Endocrinol.* **21,** 1132–1147
58. Yokoe, S., Takahashi, M., Asahi, M., Lee, S. H., Li, W., Osumi, D., Miyoshi, E., and Taniguchi, N. (2007) The Asn418-linked *N*-glycan of ErbB3 plays a crucial role in preventing spontaneous heterodimerization and tumor promotion. *Cancer Res.* **67,** 1935–1942
59. Guo, H. B., Johnson, H., Randolph, M., Lee, I., and Pierce, M. (2009) Knockdown of GnT-Va expression inhibits ligand-induced downregulation of the epidermal growth factor receptor and intracellular signaling by inhibiting receptor endocytosis. *Glycobiology* **19,** 547–559